3

FLOW PAST A CIRCULAR CYLINDER

3.1 Introduction

Relative motion between some object and a fluid is a common occurrence. Obvious examples are the motion of an aeroplane and of a submarine and the wind blowing past a structure such as a tall building or a bridge. Practical situations are, however, usually geometrically complicated. Here we wish to see the complexities of the flow that can arise even without geometrical complexity. We therefore choose a very simple geometrical arrangement, and one about which there is a lot of information available.

This is the two-dimensional flow past a circular cylinder. A cylinder of diameter d is placed with its axis normal to a flow of free stream speed u_0; that means that u_0 is the speed that would exist everywhere if the cylinder were absent and that still exists far away from the cylinder. The cylinder is so long compared with d that its ends have no effect; we can then think of it as an infinite cylinder with the same behaviour occurring in every plane normal to the axis. Also, the other boundaries to the flow (e.g. the walls of a wind-tunnel in which the cylinder is placed) are so far away that they have no effect.

An entirely equivalent situation exists when a cylinder is drawn perpendicularly to its axis through a fluid otherwise at rest. The only difference between the two situations is in the frame of reference from which the flow is being observed. (Aspects of relativity theory are already present in Newtonian mechanics.) The velocity at each point in one frame is given by the vectorial addition of u_0 onto the velocity at the geometrically similar point in the other frame (Fig. 3.1). This transformation does not change the accelerations involved or the velocity gradients giving rise to viscous forces; it thus has no effect on the dynamics of the situation. (These remarks apply only when u_0 is constant; if it is changing then one does have to distinguish between the cylinder accelerating and the fluid accelerating.)

It is, however, convenient to use a particular frame of reference for describing the flow. Except where otherwise stated, the following description will use the frame of reference in which the cylinder is at rest.

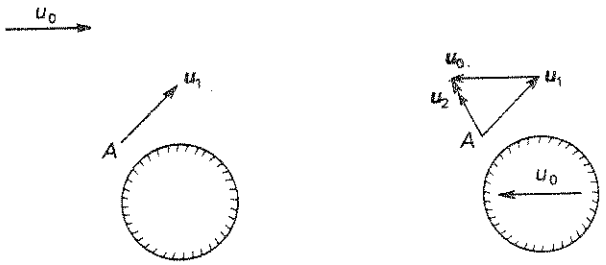

FIG. 3.1 Velocity vectors $\boldsymbol{u}_1$ and $\boldsymbol{u}_2$ at point A in two frames of reference.

3.2 The Reynolds number

One can have various values of d and u_0 and of the density, ρ, and viscosity, μ, of the fluid. For reasons like those applying to pipe flow (Section 2.4) the important parameter is the Reynolds number

$$\mathrm{Re} = \frac{\rho u_0 d}{\mu}. \tag{3.1}$$

This is the only dimensionless combination and one expects (and finds) that the flow pattern will be the same when Re is the same. We thus consider the sequence of changes that occurs to the flow pattern as Re is changed. We are concerned with a very wide range of Re. In practice this means that both u_0 and d have to be varied to make observations of the full range. For example, $\mathrm{Re} = 10^{-1}$ corresponds in air to a diameter of 10 μm with a speed of 0.15 m s^{-1} (or in glycerine to a diameter of 10 mm with a speed of 10 mm s^{-1}); $\mathrm{Re} = 10^6$ corresponds in air to a diameter of 0.3 m with a speed of 50 m s^{-1}. Thus experiments have been done with cylinders ranging from fine fibres to ones that can be used only in the largest wind-tunnels.

3.3 Flow patterns

The following description of the flow patterns is based almost entirely on experimental observations. Only for the lowest Reynolds numbers can the flow as a whole be determined analytically (Section 9.5), although there are theoretical treatments of aspects of the flow at other Reynolds numbers. Some of the flow patterns have also been studied computationally.

Figure 3.2 shows the flow when $\mathrm{Re} \ll 1$. The lines indicate the paths of elements of fluid. The flow shows no unexpected properties, but two points are worth noting for comparison with higher values of the

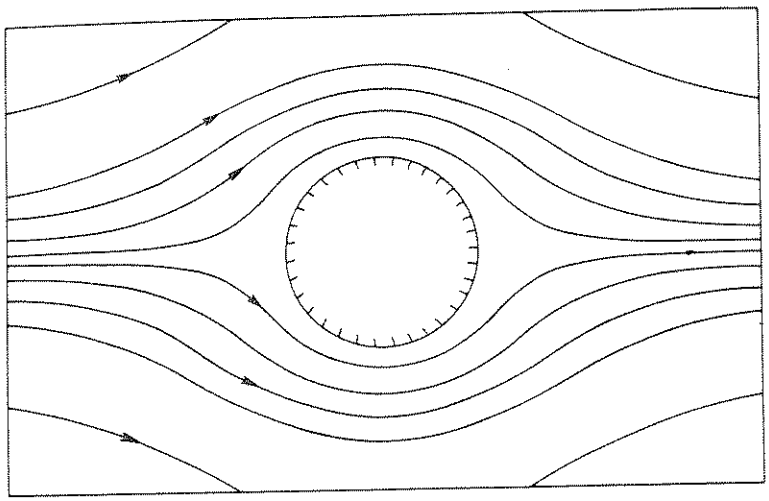

FIG. 3.2 Low Reynolds number flow past a circular cylinder.

Reynolds number. Firstly, the flow is symmetrical upstream and downstream; the right-hand half of Fig. 3.2 is the mirror image of the left-hand half. Secondly, the presence of the cylinder has an effect over large distances; even many diameters to one side the velocity is appreciably different from u_0.

As Re is increased the upstream–downstream symmetry disappears. The particle paths are displaced by the cylinder for a larger distance behind it than in front of it. When Re exceeds about 4, this leads to the feature shown in the computed flow pattern of Fig. 3.3. Fluid that comes round the cylinder close to it moves away from it before reaching the rear point of symmetry. As a result, two 'attached eddies' exist behind the cylinder; the fluid in these circulates continuously, not moving off downstream. These eddies get bigger with increasing Re [131]; Fig. 3.4 shows a photograph of the flow at $\mathrm{Re} \approx 40$ just before the next flow development takes place. (For further computed flow patterns in this regime see Section 6.2.)

The tendency for the most striking flow features to occur downstream of the cylinder becomes even more marked as one goes to higher Reynolds numbers. This region is called the wake of the cylinder. For $\mathrm{Re} > 40$ the flow in the wake becomes unsteady. As with transition to turbulence in a pipe (Section 2.6), this unsteadiness arises spontaneously even though all the imposed conditions are being held steady.

Figure 3.5 shows a sequence of patterns in a cylinder wake, produced by dye emitted through a small hole at the rear of the cylinder. The instability develops to give the flow pattern, known as a Kármán vortex

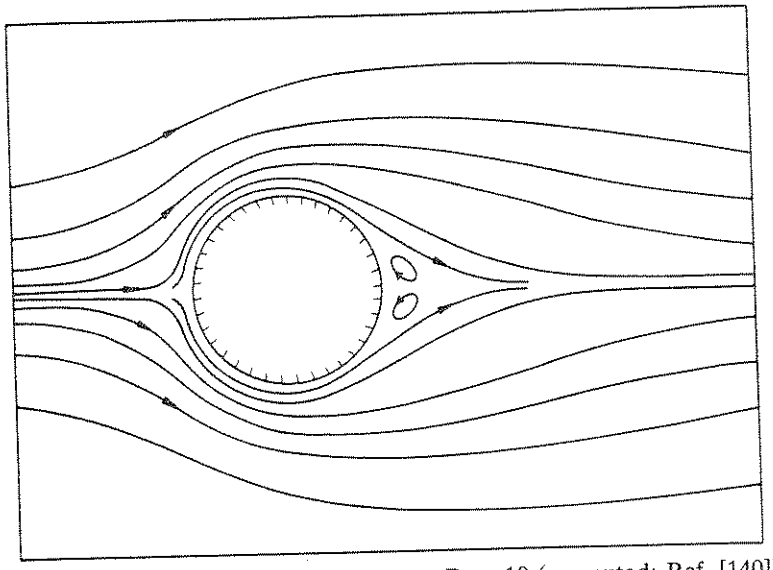

FIG. 3.3 Flow past a circular cylinder at Re = 10 (computed: Ref. [140]).

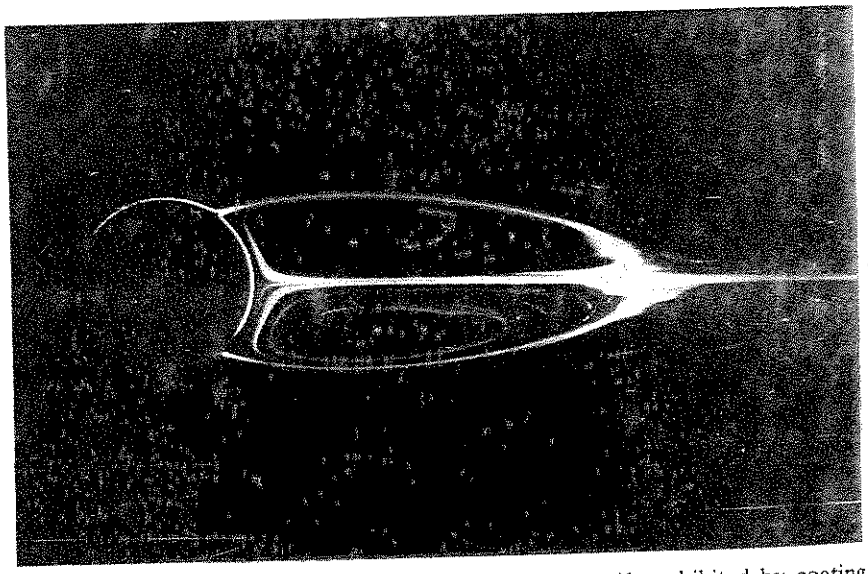

FIG. 3.4 Attached eddies on circular cylinder at Re = 41, exhibited by coating cylinder with dye (condensed milk). Ref. [364].

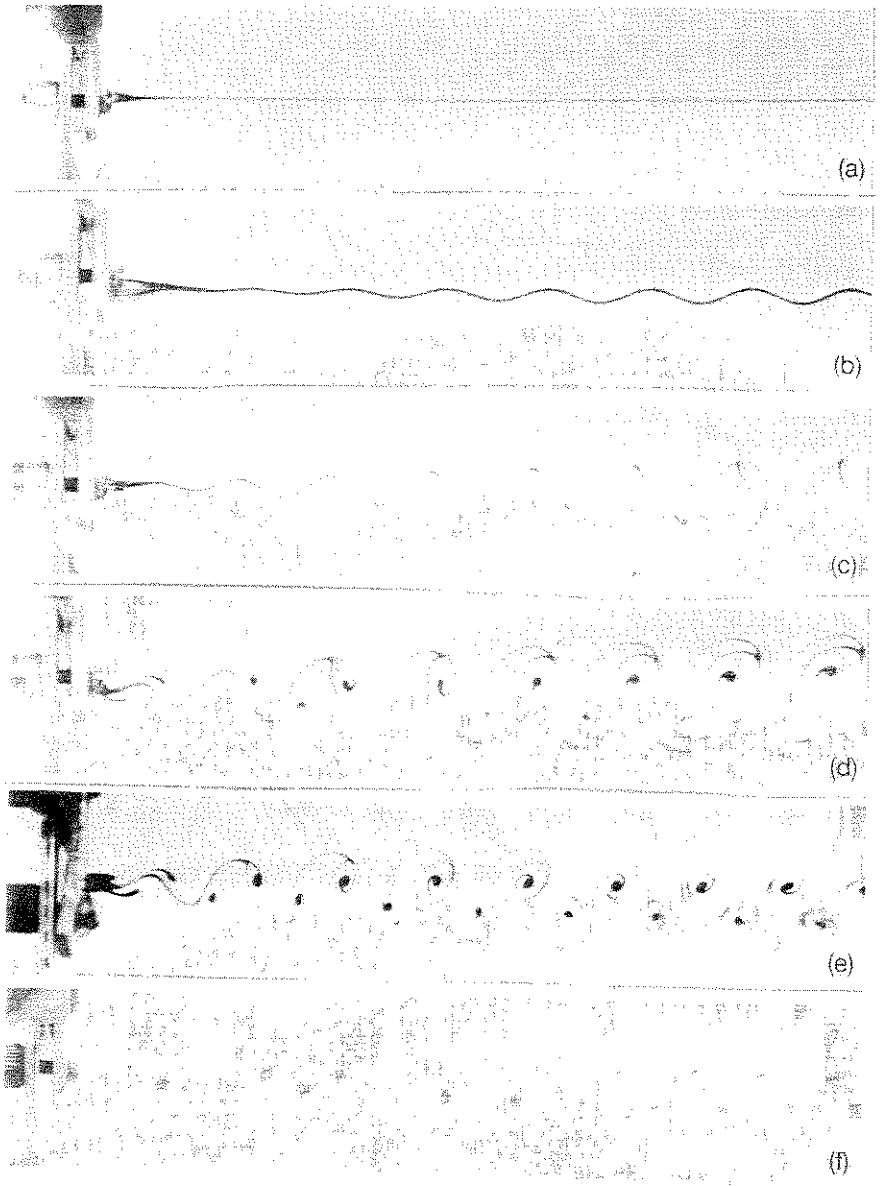

FIG. 3.5 Cylinder wakes exhibited by dye introduced through hole in cylinder. (Cylinder is obscured by bracket but can be seen obliquely, particularly in (a) and (f).) (a) Re ≈ 30; (b) Re ≈ 40; (c) Re = 47; (d) Re = 55; (e) Re = 67; (f) Re = 100.

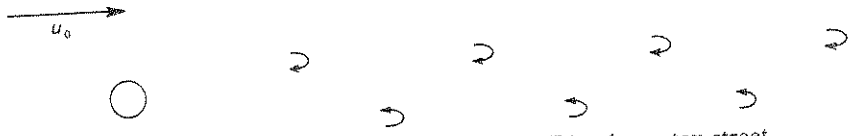

FIG. 3.6 Relative positions of vortices in Kármán vortex street.

street, shown schematically in Fig. 3.6. Concentrated regions of rapidly rotating fluid—more precisely regions of locally high vorticity (a term to be defined in Section 6.4)—form two rows on either side of the wake. All the vortices on one side rotate in the same sense, those on opposite sides in opposite senses. Longitudinally, the vortices on one side are midway between those on the other.

The whole pattern of vortices travels downstream, but with a speed rather smaller than u_0. This means that for the other frame of reference, a cylinder pulled through stationary fluid, the vortices slowly follow the cylinder. Figure 3.7 shows a photograph taken with this arrangement. A moderately long exposure shows the motion of individual particles in the fluid. Because the vortices are moving only slowly relative to the camera, the circular motion associated with them is shown well.

Vortex streets arise rather commonly in flow past obstacles (e.g. see also Sections 15.1, 17.8, 26.2, 26.8). Their basic cause is flow instability;

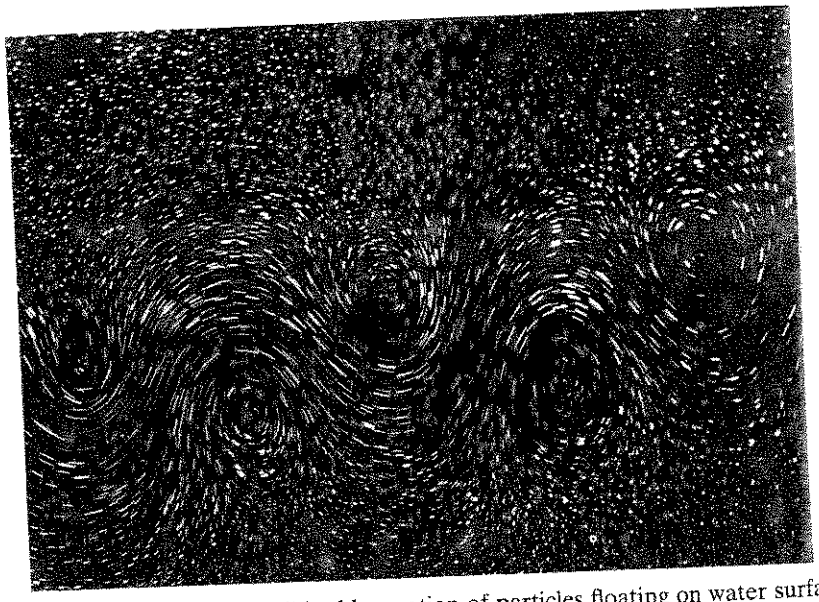

FIG. 3.7 Vortex street exhibited by motion of particles floating on water surface, through which cylinder has been drawn; Re = 200. From Ref. [380].

FIG. 3.8 Motion immediately behind cylinder; Re = 110.

the dynamics of this will be considered in Section 17.8. The process by which a vortex street is formed is often called 'eddy shedding', but this name may not always be appropriate. In the case of flow past a circular cylinder, it is applicable when the Reynolds number exceeds about 100 (Section 17.8). Then the attached eddies are periodically shed from the cylinder to form the vortices of the street. Whilst the eddy on one side is being shed, that on the other side is re-forming. Figure 3.8 shows a close-up of the region immediately behind the cylinder, with the same dye system as in Fig. 3.5, during this process.

Figure 3.9 shows a side-view of a vortex street, again shown by dye released at the cylinder. Sometimes the vortices are straight and closely parallel to the cylinder (indicating that the shedding occurs in phase all along the cylinder); sometimes they are straight but inclined to the cylinder, as in the top part of Fig. 3.9 (indicating a linear variation in the phase of shedding); and sometimes they are curved, as in the bottom part of Fig. 3.9 (indicating a more complicated phase variation). The exact behaviour is very sensitive to disturbances and so it is difficult to predict just what will occur at any given Reynolds number. One can, however, say that the lower the Reynolds number the greater is the likelihood of straight, parallel vortices.

It should be emphasized that in Figs. 3.5, 3.8, and 3.9 the introduction of dye was continuous. The gathering into discrete regions is entirely a function of the flow.

Figure 3.10 shows a sequence of oscillograms at two points fixed relative to a cylinder in a wind-tunnel as the main flow velocity is increased. In Fig. 3.10(a) and (b) it can be seen that the passage of the vortex street past the point of observation produces an almost sinusoidal variation. The frequency of this, n, is usually specified in terms of the

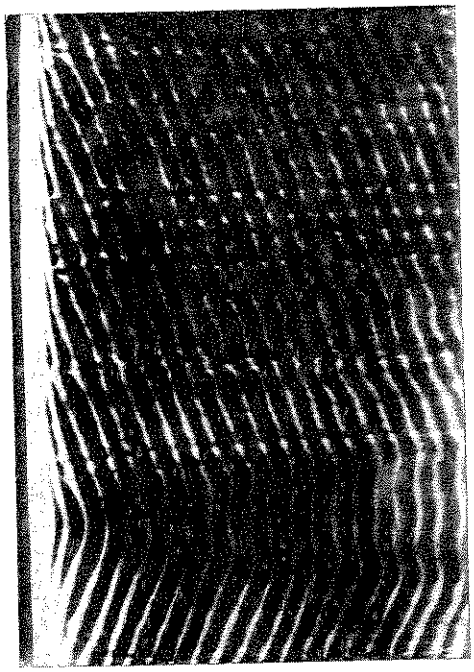

FIG. 3.9 Side-view of vortex street behind cylinder; Re = 150. From Ref. [89].

non-dimensional parameter

$$\mathrm{St} = nd/u_0 \tag{3.2}$$

known as the Strouhal number. St is a function of Re (although a sufficiently slowly varying one that it may be said that St is typically 0.2).

The remainder of Fig. 3.10 illustrates the most important aspect of what happens as the Reynolds number is further increased. The complete regularity of the fluctuations is lost. Comparison of the oscillograms at the same Reynolds number shows that the irregularities become more marked as one goes downstream. Further instabilities are leading to the breakdown of the vortex street, producing ultimately a turbulent wake such as that shown in Fig. 3.11. The term turbulent implies the existence of highly irregular rapid velocity fluctuations, in the same way as in Section 2.6. The turbulence is confined to the long narrow wake region downstream of the cylinder. The character of a turbulent wake will be discussed in more detail in Sections 21.3 and 21.4.

The transition to turbulent motion is a consequence of further instabilities [95], which will be considered more fully in Section 17.8. In summary, there are two important types of instability: one occurring

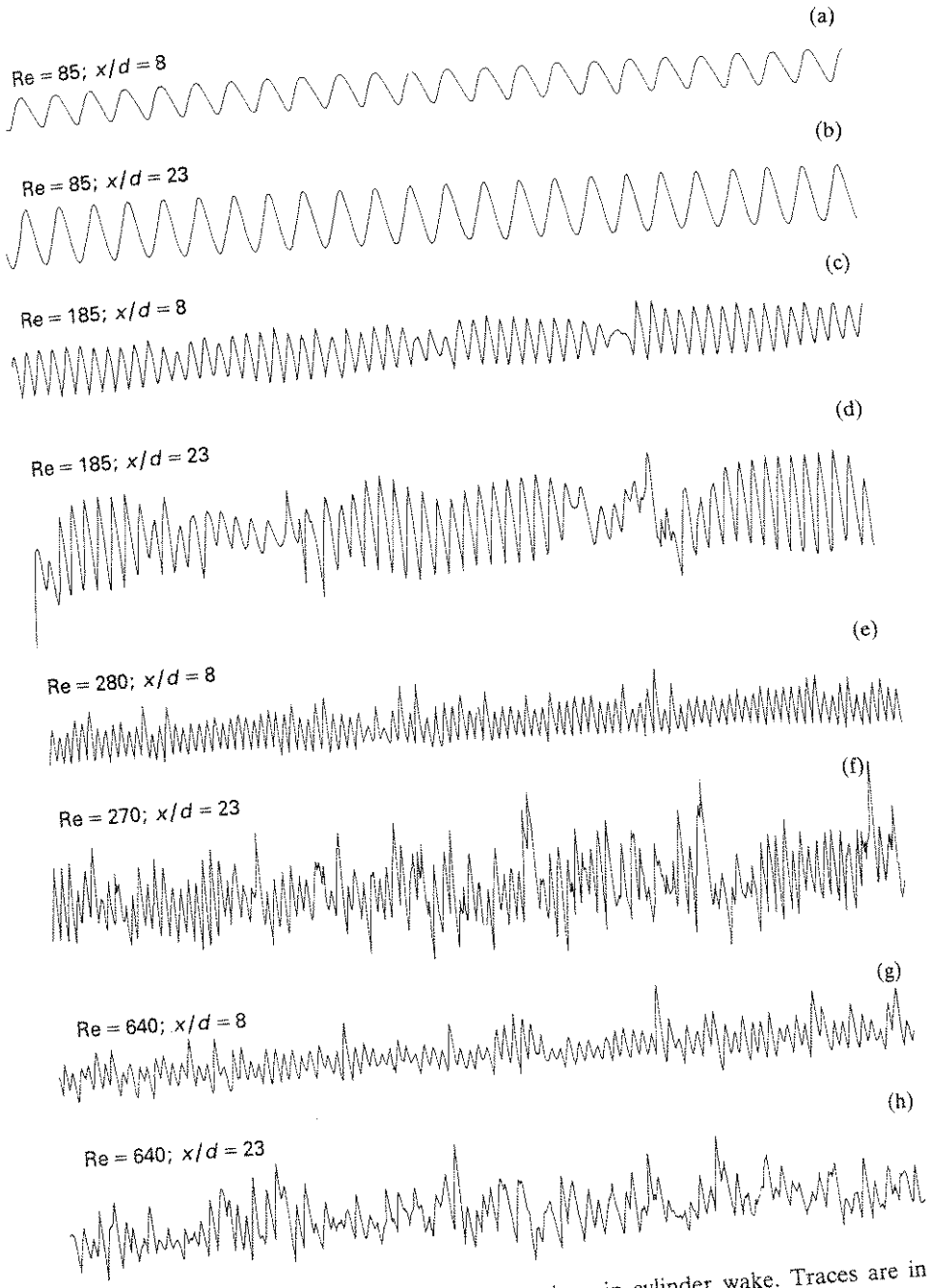

FIG. 3.10 Oscillograms of velocity fluctuations in cylinder wake. Traces are in pairs at same Re, but different distances, x, downstream from cylinder. For both positions, probe was slightly off-centre to be influenced mainly by vortices on one side of street. (Notes: relative velocity amplitudes are arbitrary; time scale is expanded by factor of about 3 in traces (g) and (h).)

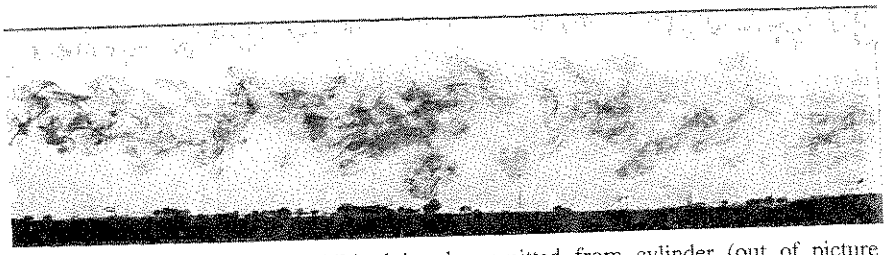

FIG. 3.11 Turbulent wake exhibited by dye emitted from cylinder (out of picture to right). From Ref. [186].

when the Reynolds number exceeds about 200 and acting three-dimensionally on the vortex street as a whole; the other occurring when Re exceeds about 400 and originating just downstream of the points of flow separation from the cylinder (Fig. 3.12). Because the latter occurs further upstream it is the primary cause of transition once $\mathrm{Re} > 400$. In fact there is a wide range of Reynolds number, from this value up to about 3×10^5, in which, although there are changes in details of the flow [95, 175, 297], the broad picture, of a primary instability producing a vortex street and a secondary one disrupting this to give a turbulent wake, remains the same.

At $\mathrm{Re} \approx 3 \times 10^5$, a dramatic development occurs. To understand this we must first consider developments at lower Re at the front and sides of the cylinder. There the phenomenon known as boundary layer formation

FIG. 3.12 Flow past cylinder at $\mathrm{Re} = 4800$. High-speed schlieren (Section 25.4) photography with small density difference produced in air flow by introducing a small amount of carbon dioxide at cylinder surface. From Ref. [230].

occurs. This will be the subject of a full discussion later in the book (Section 8.3 and Chapter 11). For the moment, we may just say that there is a region, called the boundary layer, next to the wall of the cylinder in which all the changes to the detailed flow pattern occur. Outside this the flow pattern is independent of the Reynolds number. For these statements to mean anything, the boundary layer must be thin compared with the diameter of the cylinder; this is the case when Re is greater than about 100. (Boundary layer formation does not start by a sudden transition of the sort we have been considering previously; it is an asymptotic condition approached at high enough Re. The figure of 100 is just an order of magnitude.)

The change in the flow at $\mathrm{Re} \approx 3 \times 10^5$ results from developments in the boundary layer. Below this Reynolds number the motion there is laminar. Above, it undergoes transition to turbulence. At first, this transition takes a rather complicated form [157, 325]: laminar fluid close to the wall moves away from it as if it were entering the attached eddies; transition then occurs very quickly and the turbulent flow reattaches to the wall only a small distance downstream from the laminar separation. (See Section 12.6 for more precise consideration of these processes.) There are also complications due to the facts that the transition can occur asymmetrically between the two sides of the cylinder [157] and non-uniformly along its length [157, 203].

At higher values of the Reynolds number, above about 3×10^6, transition occurs in the boundary layer itself, thus eliminating the laminar separation and turbulent reattachment. The transition process is now similar to that described for pipe flow.

Whether or not it has previously undergone laminar separation and turbulent reattachment, the turbulent boundary layer itself separates; the fluid in it moves away from the wall of the cylinder and into the wake some distance before the rear line of symmetry. This occurs, however, much further round the cylinder than when the boundary layer remains laminar (Fig. 3.13). As a result the wake is narrower for $\mathrm{Re} > 3 \times 10^5$ than for $\mathrm{Re} < 3 \times 10^5$. When $\mathrm{Re} > 3 \times 10^5$, the fluid entering the wake is already turbulent and so the transition process immediately behind the cylinder is eliminated.

Markedly periodic vortex shedding remains a characteristic of the flow up to the highest Reynolds number ($\sim 10^7$) at which observations have been made. When this is not immediately apparent from oscillograms like Fig. 3.10, Fourier analysis reveals the presence of a dominant frequency amongst the other more random fluctuations. There are in fact two ranges, $200 < \mathrm{Re} < 400$ and $3 \times 10^5 < \mathrm{Re} < 3 \times 10^6$, in which the regularity of shedding decreases: in the former the Strouhal number shows a lot of scatter; in the latter the periodicity is lost except very close behind

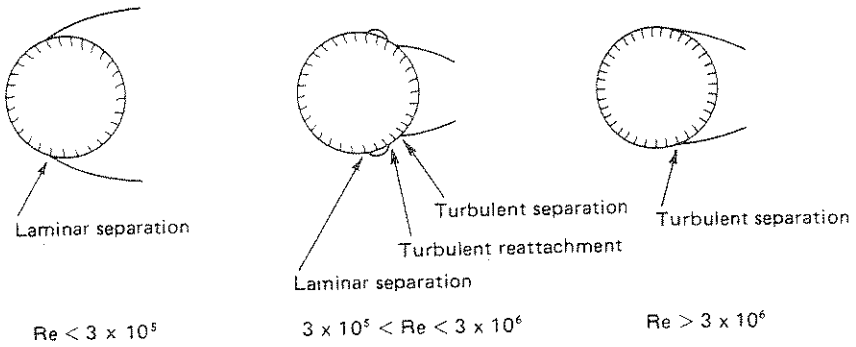

FIG. 3.13 Separation positions for various Reynolds number ranges.

the cylinder [90, 325]. The ends of these ranges can be identified with changes in the flow discussed above. At the top end of each range the change restores the regularity which had been lost at the bottom end; the Strouhal number becomes well defined again.

3.4 Drag

An important quantity associated with the relative motion between a body and a fluid is the force produced on the body. One has to apply a force in order to move a body at constant speed through a stationary fluid. Correspondingly an obstacle placed in a moving fluid would be carried away with the flow if no force were applied to hold it in place. The force in the flow direction exerted by the fluid on an obstacle is known as the drag. There is an equal and opposite force exerted by the obstacle on the fluid.

At high Reynolds numbers, this can be thought of as the physical mechanism of wake formation. Because of the force between it and the obstacle, momentum is removed from the fluid. The rate of momentum transport downstream must be smaller behind the obstacle than in front of it. There must thus be a reduction in the velocity in the wake region (Fig. 3.14). (At low Reynolds numbers, when the velocity and pressure are modified to large distances on either side of the obstacle, the situation is more complex.)

For the circular cylinder the important quantity is the drag per unit length; we denote this by D. It is conventional to present results for D in terms of the drag coefficient, defined as

$$C_D = \frac{D}{\frac{1}{2}\rho u_0^2 d}. \tag{3.3}$$

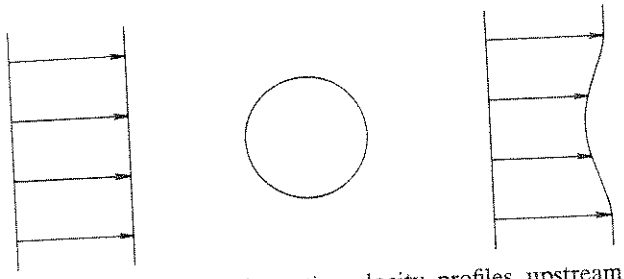

FIG. 3.14 Wake production: schematic velocity profiles upstream and downstream of an obstacle.

This anticipates ideas to be introduced in Chapter 7. It is plausible ahead of that discussion that, since the Reynolds number is being used to specify the conditions, results for D should be presented non-dimensionally; C_D is non-dimensional. This procedure does in fact enable all conditions to be covered by a single curve, shown in Fig. 3.15. The curve is based primarily on experimental measurements, too numerous to show individual points. At the low Re end the experiments can be matched to theory.

The corresponding plot between Reynolds number and drag coefficient can also be given for a sphere, although with less precision because of the experimental problem of supporting the sphere. The curve, although different in detail, shows all the same principal features as the one for the cylinder.

A few features of the curves merit comment, some of these being points to which we shall return in later chapters.

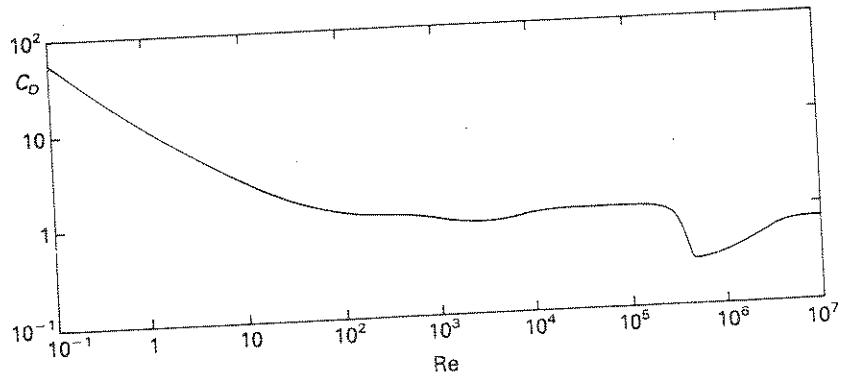

FIG. 3.15 Variation of drag coefficient with Reynolds number for circular cylinder. Curve is experimental, based on data in Refs. [139, 159, 325, 370, 386, 410]. See also Refs. [204, 211].

At low Reynolds numbers,

$$C_D \propto \frac{1}{\mathrm{Re}}. \tag{3.4}$$

(This is actually an accurate representation for the sphere, an approximate one for the cylinder—see Sections 9.4 and 9.5.) For a given body in a given fluid (fixed d, ρ, and μ) this corresponds to

$$D \propto u_0. \tag{3.5}$$

Direct proportionality of the drag to the speed is a characteristic behaviour at low speeds.

Over a wide range of Reynolds number (10^2 to 3×10^5) the drag coefficient varies little. For a given body in a given fluid, constant C_D corresponds to

$$D \propto u_0^2. \tag{3.6}$$

Proportionality of the drag to the square of the speed is often a characteristic behaviour at high speeds.

However, there is a dramatic departure from this behaviour at $\mathrm{Re} \approx 3 \times 10^5$. The drag coefficient drops by a factor of over 3. This drop occurs sufficiently rapidly that there is actually a range over which an increase in speed produces a decrease in drag. We have seen that this Reynolds number corresponds to the onset of turbulence in the boundary layer. The consequent delayed separation of the boundary layer results in a narrower wake. Since this in turn corresponds to less momentum extraction from the flow, one might expect the lower drag. The result is nonetheless a somewhat paradoxical one since transition to turbulence usually produces an increased drag. In fact, on the cylinder and sphere, the force exerted directly by the boundary layer does increase on transition. But this is more than counteracted by another effect: changes in the pressure distribution over the surface. This will be discussed more fully in Section 12.5.